Advances in Aircraft and Spacecraft Science, *Vol. 5, No. 2 (2018) 259-275*
DOI: https://doi.org/10.12989/aas.2018.5.2.259

Static and dynamic load superposition in spacecraft structural analysis

Xavier Vaquer-Araujo*, Florian Schöttle[a], Andreas Kommer[b] and Werner Konrad[c]

Airbus DS GmbH Friedrichshafen, Claude-Dornier-Straße, 88039 Friedrichshafen, Germany

(Received December 16, 2016, Revised September 14, 2017, Accepted November 6, 2017)

Abstract. In mechanical analysis of spacecraft structures situations appear where static and dynamic loads must be considered simultaneously. This could be necessary either by load definition or preloaded structures. The superposition of these environments has an impact on the load and stress distribution of the analysed structures. However, this superposition cannot be done by adding both load contributions directly. As an example, to compute equivalent Von Mises stresses, the phase information must be taken into account in the stress tensor superposition. Finite Element based frequency response solvers do not allow the calculation of superposed static and dynamic responses. A manual combination of loads in a post-processing task is required. In this paper, procedures for static and harmonic loads superposition are presented and supported by analytical and finite element-based examples. The aim of the paper is to provide evidence of the risks of using different superposition techniques. Real application examples such as preloaded mechanism structures and propulsion system tubing assemblies are provided. This study has been performed by the Structural Engineering department of Airbus Defence and Space GmbH Friedrichshafen.

Keywords: load superposition; structural dynamics; phase; static preload; spacecraft

1. Introduction

Spacecraft structures are designed to survive all events that occur during launch and in-orbit phases. These events are mainly of dynamic nature. It is therefore necessary to know and understand the spacecraft's dynamic characteristics to produce a compliant and optimised design.
During mechanical analysis tasks, loads are usually combined to obtain critical or equivalent loads. These loads are afterwards used to size the structure. Special attention must be paid on the way the load combination is performed in order not to yield very conservative or non-conservative results. For example, the phase of the responses is a key factor to be considered when combining dynamic loads in order to obtain accurate results.

In addition, statically preloaded structures such as mechanisms introduce a new element into

*Corresponding author, Structural Engineer, E-mail: xavier.vaqueraraujo@airbus.com
[a]Structural Engineering Department Team Leader, E-mail: florian.schoettle@airbus.com
[b]Structural Engineering Department Technical Authority, E-mail: andreas.kommer@airbus.com
[c]Head of Structural Engineering Department, Ph.D., E-mail: werner.konrad@airbus.com

http://www.techno-press.org/?journal=aas&subpage=7 ISSN: 2287-528X (Print), 2287-5271 (Online)

the equation: static loads. These loads may be present during the launch phase of the spacecraft and therefore need to be included in addition to the dynamic environmental loads. The procedure followed to derive the superposed responses is critical.

In the framework of harmonic environment, this paper introduces and compares several dynamic response combination techniques as well as different methodologies of static and dynamic load superposition. The aim of the paper is to provide evidence of the risks of using each technique. To this end, theoretical and FEM based examples are provided.

The structure of the paper is as follows. Section 2 provides a description of the FEM benchmark model used for this study. Sec. 3 reviews key aspects to be considered for accurate combination of dynamic responses. In sec. 4, techniques for static and dynamic loads superposition are presented and compared. Sec. 5 provides examples of application in spacecraft programmes developed in Airbus DS GmbH Friedrichshafen. Finally, future perspectives and conclusions are drawn in sec. 6 and sec. 7.

2. Benchmark model

For simplification and better understanding of the results of this study, a typical benchmark Finite Element (FE) model consisting of a beam with a large tip mass is used. As depicted in Fig. 1, the beam is a circular tube modelled with 2D shell elements. A lumped mass is attached to the tip of the beam with a rigid element RBE2 spider. The global Z direction is parallel to the beam longitudinal axis.

The elements highlighted in pink will be used in sec. 3 and sec. 4 to present stress results.

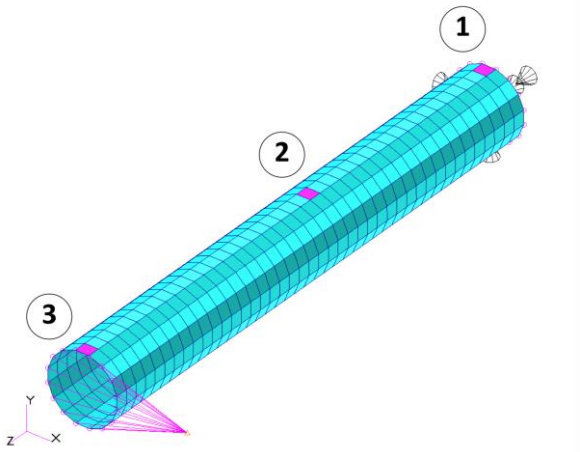

Fig. 1 Overview of the Benchmark FE Model

The modal properties under hard-mounted boundary conditions applied at the end of the beam opposite to the mass are summarised in Table 1. Since solely excitation in Y direction is analysed in this paper, only modes in Y direction are of interest. The shapes of the three first modes in Y direction are depicted in Fig. 2.

Table 1 Benchmark FEM modal properties

Mode N°	Frequency	Description
Mode 1	8.44 Hz	1st Bending Mode in Y
Mode 2	11.13 Hz	2nd Bending Mode in Y + Torsion Z
Mode 3	32.76 Hz	3rd Bending Mode in Y

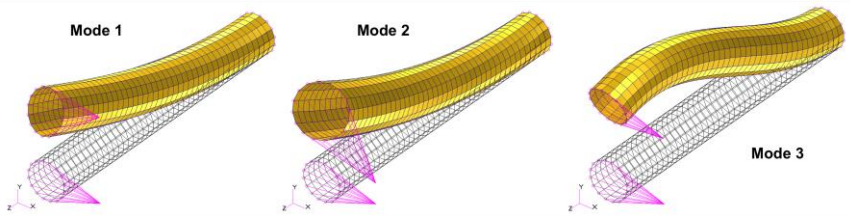

Fig. 2 Benchmark FEM Mode Shapes

3. Dynamic load combination

In harmonic analysis, amplitude and phase of responses are calculated solving the equations of motion. Once the responses are calculated, it is usual to combine them to produce, for instance, equivalent Von Mises stress or in-plane loads. In order to simplify the calculations, analysts sometimes take the risk to ignore the phase of the responses and work with amplitudes only. The aim of this section is to provide evidence that the phase information must be included when combining dynamic responses since ignoring it may yield very conservative or non-conservative results.

3.1 Example 1

As an example, consider the following 2D dynamic stress tensor

$$[\sigma]=\begin{bmatrix}\sigma_x(t) & \tau_{xy}(t)\\ & \sigma_y(t)\end{bmatrix}=\begin{bmatrix}|\sigma_x|\cos(\omega t+\phi_x) & |\tau_{xy}|\cos(\omega t+\phi_{xy})\\ & |\sigma_y|\cos(\omega t+\phi_y)\end{bmatrix} \tag{1}$$

where $|\sigma_i|$, $|\tau_{ij}|$ are normal and shear stress amplitudes and ϕ_i, ϕ_{ij} are response initial phases.

The exact Von Mises stress is calculated as in Eq. (2)

$$\sigma_{vm}(t)=\sqrt{\sigma_x(t)^2+\sigma_y(t)^2-\sigma_x(t)\sigma_y(t)+3\tau_{xy}(t)^2} \tag{2}$$

Eq. (2) is a periodic function of period $\theta=\omega t\in[0,\pi)$ where ω is the circular frequency of excitation. Developing Eq. (2) using Eq. (1), one yields an exact expression to determine the value of $\theta=\omega t$ for which Eq. (2) reaches a maximum or a minimum value (Charron *et al*. 1993)

$$-\tan(2\theta)=\frac{|\sigma_x|^2\sin(2\phi_x)+|\sigma_y|^2\sin(2\phi_y)+3|\tau_{xy}|^2\sin(2\phi_{xy})-|\sigma_x||\sigma_y|\sin(\phi_x+\phi_y)}{|\sigma_x|^2\cos(2\phi_x)+|\sigma_y|^2\cos(2\phi_y)+3|\tau_{xy}|^2\cos(2\phi_{xy})-|\sigma_x||\sigma_y|\cos(\phi_x+\phi_y)} \tag{3}$$

If one decides to neglect the phase of the responses in order to simplify the dynamic Von Mises stress calculation one leads to Eq. (4)

$$\sigma_{vm\ amp} = \sqrt{|\sigma_x|^2 + |\sigma_y|^2 - |\sigma_x||\sigma_y| + 3|\tau_{xy}|^2} \tag{4}$$

As an example, let us consider the 2D stress tensor displayed in Table 2. With this tensor, one can plot the dynamic 2D stress tensor of Eq. (1) together with the Von Mises stress calculated with Eqs. (2) and (4) as depicted in Fig. 3.

Table 2 Dynamic 2D stress tensor example

$\lvert\sigma_x\rvert$ [MPa]	ϕ_x [rad]	$\lvert\sigma_y\rvert$ [MPa]	ϕ_y [rad]	$\lvert\tau_{xy}\rvert$ [MPa]	ϕ_{xy} [rad]
200	$\pi/2$	200	$3\pi/2$	80	$\pi/4$

Fig. 3 shows the exact dynamic Von Mises stress over a period $\theta = \omega t \in [0, 2\pi)$. Using Eq. (3), one exactly obtains that the maximum Von Mises stress is located at $\theta = 1.65$ rad. In addition, the Von Mises stress neglecting the phase of the responses (Eq. (4)) is depicted in black solid line.

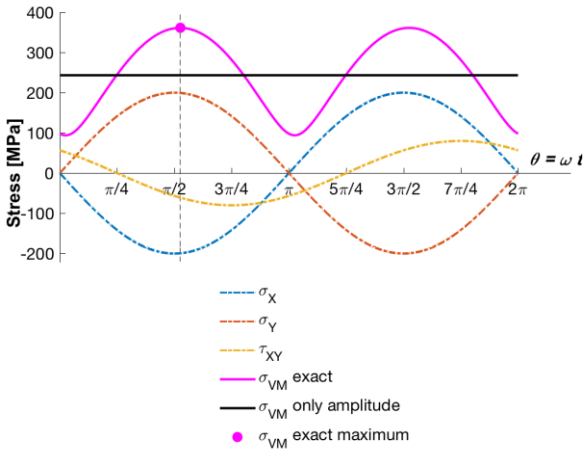

Fig. 3 Example of dynamic Von Mises stress

Using Eq. (5), one can compute the percentage of error committed when neglecting the phase of the responses (see Table 3).

$$e_{vm}[\%] = \frac{\sigma_{vm\ amp} - \sigma_{vm\ exact\ max}}{\sigma_{vm\ exact\ max}} \cdot 100 \tag{5}$$

Table 3 Error in dynamic Von Mises stress calculation

$\sigma_{vm\ exact\ max}$ [MPa]	$\sigma_{vm\ amp}$ [MPa]	e_{vm} [%]
361	243	-33

It can be clearly noted in Table 3 that neglecting the phase information for the Von Mises stress calculation leads to very non-conservative results.

3.2 Example 2

In a similar way, consider the following force vector

$$\vec{F} = \begin{Bmatrix} F_x(t) \\ F_y(t) \end{Bmatrix} = \begin{Bmatrix} |F_x| \cos(\omega t + \phi_x) \\ |F_y| \cos(\omega t + \phi_y) \end{Bmatrix} \tag{6}$$

where $|F_i|$ are force amplitudes and ϕ_i are response initial phases.

Very often forces are combined to obtain, for example, in-plane resultant forces as shown in Eq. (7)

$$F_R(t) = \sqrt{F_x(t)^2 + F_y(t)^2} \tag{7}$$

Combining Eqs. (6) and (7) one can obtain an exact expression to determine the value of $\theta = \omega t$ for which Eq. (7) reaches a maximum or minimum value

$$-\tan(2\theta) = \frac{|F_x|^2 \sin(2\phi_x) + |F_y|^2 \sin(2\phi_y)}{|F_x|^2 \cos(2\phi_x) + |F_y|^2 \cos(2\phi_y)} \tag{8}$$

If one decides to neglect the phase of the responses so as to simplify the dynamic in-plane resultant force calculation, one leads to Eq. (9)

$$F_{R\ amp} = \sqrt{|F_x|^2 + |F_y|^2} \tag{9}$$

As an example, let us consider the force vector displayed in Table 4. With this vector, one can plot the dynamic force vector of Eq. (6) together with the in-plane resultant force calculated with Eqs. (7) and (9) as depicted in Fig. 4.

Table 4 Dynamic Force vector example

$\lvert F_x \rvert$ [N]	ϕ_x [rad]	$\lvert F_y \rvert$ [N]	ϕ_y [rad]
1000	0	8	$\pi/2$

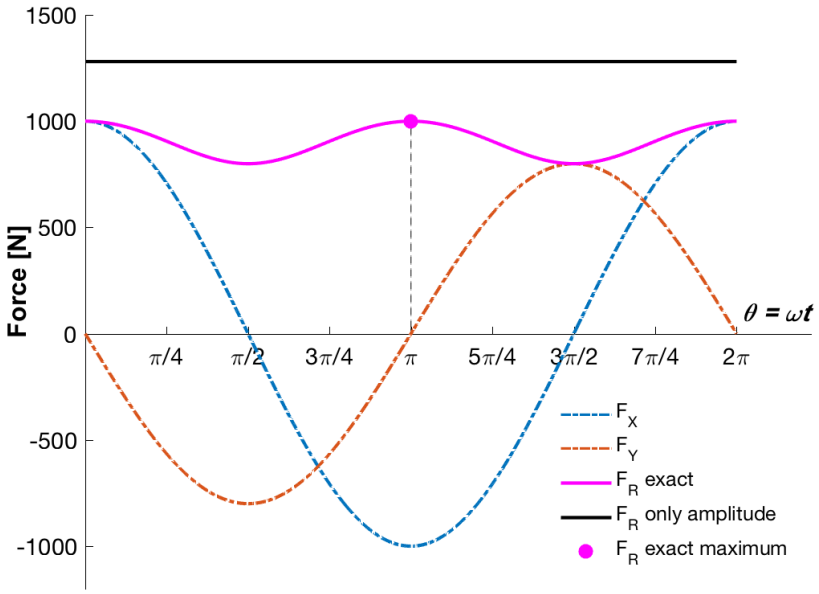

Fig. 4 Example of dynamic resultant force

Fig. 4 shows the exact in-plane resultant force over a period $\theta = \omega t \in [0, 2\pi)$. Using Eq. 8, the maximum exact resultant force is located at $\theta = \pi$ rad. In addition, in black solid line, the resultant in-plane force neglecting the phase information (Eq. (9)) is depicted.

Using Eq. (10), one can compute the percentage of error committed when neglecting the phase of the responses (see Table 5).

$$e_F[\%] = \frac{F_{R\ amp} - F_{R\ exact\ \max}}{F_{R\ exact\ \max}} \cdot 100 \tag{10}$$

Table 5 Error in dynamic resultant force calculation

$F_{R\ exact\ \max}$ [N]	$F_{R\ amp}$ [N]	e_F [%]
1000	1281	+28

From Table 5, one can conclude that ignoring the phase information is leading to a very conservative result.

Additionally, it can be demonstrated that considering only force response amplitudes is always a conservative approach. Let us consider the force vector cases listed in Table 6. If we vary the phases ϕ_x and ϕ_y such as we cover $(\phi_y - \phi_x) \in [0, \pi/2]$, then one can plot Eq. (7) as a function of $F_x(t)$ and $F_y(t)$ for one period of $\theta = \omega t \in [0, 2\pi)$ as depicted in Fig. 5.

Table 6 Force vector demonstration cases

Case	$\lvert F_x \rvert$ [N]	$\lvert F_y \rvert$ [N]
$\lvert F_x \rvert = \lvert F_y \rvert$	100	100
$\lvert F_x \rvert \neq \lvert F_y \rvert$	100	90

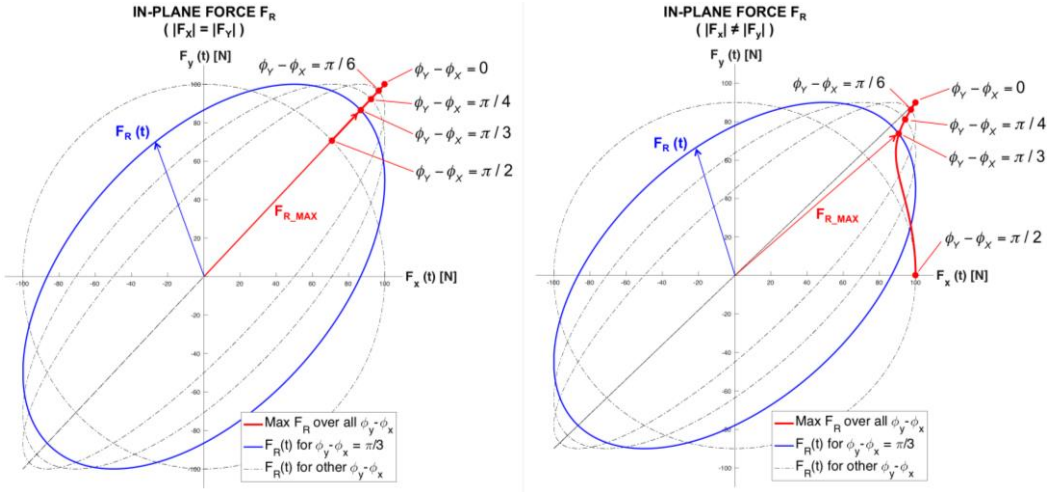

Fig. 5 Resultant in-plane force for cases $\lvert F_x \rvert = \lvert F_y \rvert$ and $\lvert F_x \rvert \neq \lvert F_y \rvert$

The ellipses depicted in Fig. 5 represent the trace of the resultant in-plane force (Eq. (7)) over a period of $\theta = \omega t$ and for several combinations of ϕ_x and ϕ_y. The blue curve depicts an example of resultant ellipse for a phase difference $(\phi_y - \phi_x)$ of $\pi/3$. The red curve shows the trail of the maximum in-plane resultant force $F_{R\ exact\ \max}$ for all possible $(\phi_y - \phi_x)$ combinations between 0 and $\pi/2$. Note that in the case $\lvert F_x \rvert \neq \lvert F_y \rvert$ the resultant ellipse rotates when $(\phi_y - \phi_x)$ increases.

It can be clearly seen that $F_{R\ exact\ \max}$ does always reach its maximum when $F_x(t)$ and $F_y(t)$ are in phase (meaning $\phi_y - \phi_x = 0$). This particular case is equivalent to neglecting the phase information as assumed in Eq. (9).

Hence, when calculating resultant forces, one will always be conservative if the phase of responses is ignored. Nevertheless, the degree of conservatism can be very high as seen in Table 5.

3.3 Benchmark example

The goal of this subsection is to provide numerical evidence of the errors in the Von Mises stress calculation when neglecting the phase information of the stress tensor.

Consider the beam finite element benchmark model presented in sec. 2. The structure is

submitted to a harmonic base excitation applied in Y direction as shown in Fig. 6. A stress analysis is performed on the tube. For simplification, only the stress tensor and Von Mises stresses on the pink elements are presented. The Von Mises stress distribution of the beam for the first three modes in Y direction is depicted in Fig. 7.

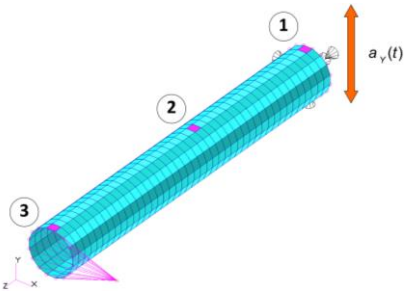

Fig. 6 Overview of Benchmark FEM with base excitation in Y direction

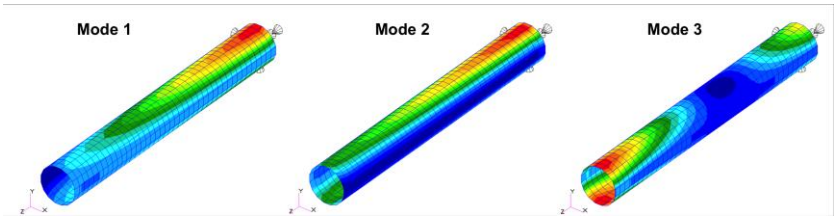

Fig. 7 Von Mises stress distribution for the three first modes in Y direction

Table 7 shows the stress tensor and Von Mises stress results for the sine Y excitation. The exact maximum Von Mises stress is calculated with Eqs. (2) and (3). The simplified Von Mises stress using Eq. (4) is presented as well. The error is computed according to Eq. (5) and is also shown in Table 7. Fig. 8 depicts the evolution of the Von Mises stress over one period of $\theta = \omega t$ for the three elements indicated in Fig. 6.

Table 7 Benchmark example dynamic Von Mises stress results overview

Mode	Element	$\lvert\sigma_x\rvert$ [MPa]	ϕ_x [deg]	$\lvert\sigma_y\rvert$ [MPa]	ϕ_y [deg]	$\lvert\tau_{xy}\rvert$ [MPa]	ϕ_{xy} [deg]	σ_{vm} exact [MPa]	σ_{vm} only amplitude [MPa]	Error e_{vm} [%]
1	1	418	-89.1	16.5	91.0	83.5	-91.3	450	435	-3.46
	2	316	-89.6	1.10	92.3	91.5	-91.0	354	353	-0.27
	3	141	-91.7	5.70	88.3	83.5	-91.3	204	200	-1.95
2	1	79.6	-121.2	23.9	-121.2	38.2	104.2	89.4	96.9	+8.34
	2	64.8	-122.6	0.08	-114.3	37.7	-104.8	84.2	91.9	+9.18
	3	53.5	-124.9	0.21	69.0	38.2	104.2	77.8	84.9	+9.16
3	1	191	-90.8	8.44	89.3	6.79	92.4	195	187	-4.31
	2	15.5	97.7	1.95	-90.2	6.79	92.4	20.3	18.7	-7.50
	3	275	90.2	11.2	-89.8	6.81	92.4	281	270	-3.98

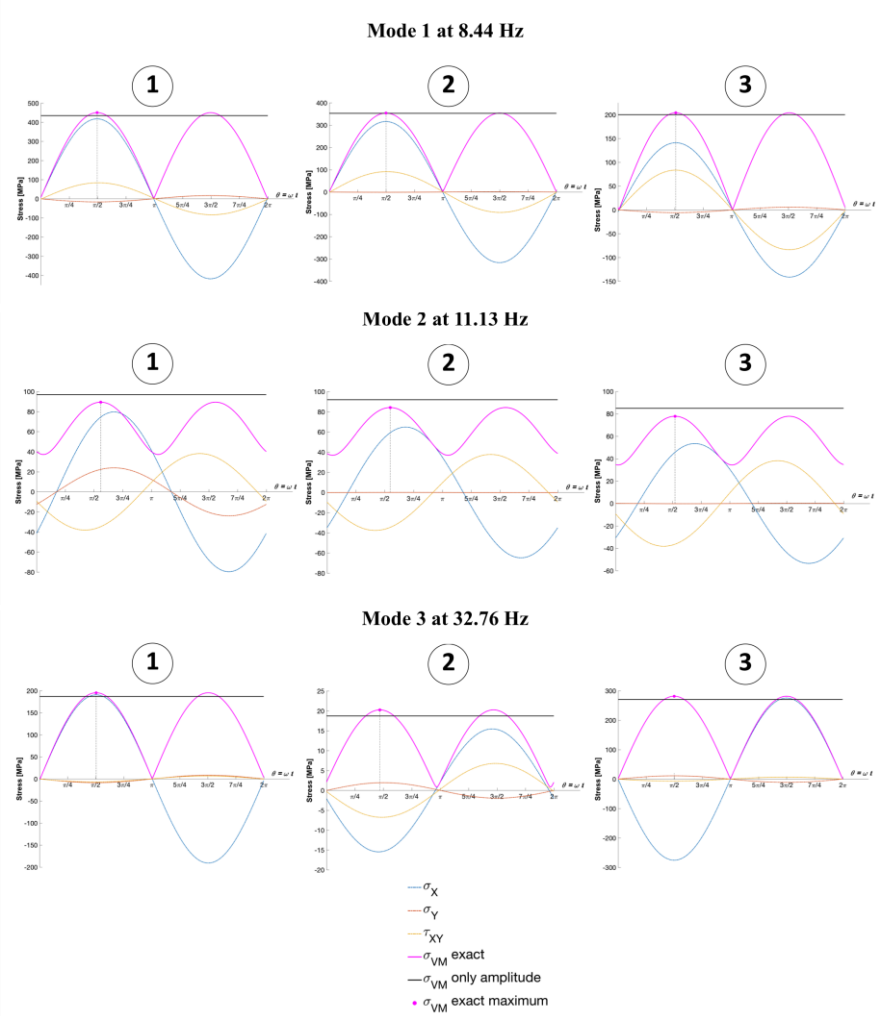

Fig. 8 Plot over one period of the FEM dynamic stress tensors and Von Mises stress

3.4 Discussion on the dynamic load combination

Both analytical and benchmark examples prove that ignoring the phase information of the responses has a high impact in the resultant force and Von Mises stress calculation. Example 2 demonstrates that neglecting the phase is always conservative when calculating resultant forces although the degree of conservatism can be very high.

In the benchmark example, errors up to 9% in Von Mises stress are achieved but the analytical example shows that even much higher errors can be made (e.g., Example 1 with an error of -33%). Table 7 provides evidence that in some cases the Von Mises calculation is conservative whereas in other cases it is non-conservative. This uncertainty in the results can be critical when sizing structures. Depending on the component and its degree of optimisation, an under-estimated Von Mises stress may lead to positive margins of safety in the analysis but to failure of the component during environmental tests.

Hence, despite the complexity of the structure and the size of the mathematical models, it is recommended to use exact methodologies of dynamic load combination which take into account the phase of the responses.

4. Superposition of static and dynamic loads

As already stated in sec. 1, there are situations where spacecraft structures are simultaneously submitted to static and dynamic environments. As an example, pointing mechanisms are required to be fixed in stowed configuration during the launch phase. Usually, this requirement is satisfied by the introduction of a static preload in the structure. Such preload may reach values of tens of kN and therefore have a strong impact in the dimensioning of the structure.

Consider the following stress tensor derived from applying a static preload

$$[\hat{\sigma}] = \begin{bmatrix} \hat{\sigma}_x & \hat{\tau}_{xy} \\ & \hat{\sigma}_y \end{bmatrix} \tag{11}$$

The Von Mises stress of this static tensor would be as in Eq. (12)

$$\hat{\sigma}_{vm\ static} = \sqrt{\hat{\sigma}_x{}^2 + \hat{\sigma}_y{}^2 - \hat{\sigma}_x\hat{\sigma}_y + 3\hat{\tau}_{xy}{}^2} \tag{12}$$

Assume that static loads must be applied in combination with dynamic environmental loads. In that case, the stress tensor in Eq. (11) and the dynamic stress tensor displayed in Eq. (1) have to be superposed

$$\begin{aligned} [\bar{\sigma}] &= \begin{bmatrix} \bar{\sigma}_x(t) & \bar{\tau}_{xy}(t) \\ & \bar{\sigma}_y(t) \end{bmatrix} = \begin{bmatrix} \hat{\sigma}_x + \sigma_x(t) & \hat{\tau}_{xy} + \tau_{xy}(t) \\ & \hat{\sigma}_y + \sigma_y(t) \end{bmatrix} = \\ &= \begin{bmatrix} \hat{\sigma}_x + |\sigma_x|\cos(\omega t + \phi_x) & \hat{\tau}_{xy} + |\tau_{xy}|\cos(\omega t + \phi_{xy}) \\ & \hat{\sigma}_y + |\sigma_y|\cos(\omega t + \phi_y) \end{bmatrix} \end{aligned} \tag{13}$$

At this point, one can observe that the static and dynamic superposition shown in Eq. (13) is not straightforward. FE based dynamic solutions cannot include static loads in the solution sequence and therefore the superposition must be done as a post-processing task.

Consider that we desire to compute the exact Von Mises stress of the static and dynamic superposed tensor of Eq. (13). The exact procedure is presented in Eqs. (14) and (15)

$$\forall\, elements, \forall\, \omega \in \Omega, \forall\, \theta = \omega t \in [0, 2\pi) \rightarrow \max[\bar{\sigma}_{vm}(t)] \tag{14}$$

with Ω the frequency range of analysis and

$$\bar{\sigma}_{vm}(t) = \sqrt{[\hat{\sigma}_x + \sigma_x(t)]^2 + [\hat{\sigma}_y + \sigma_y(t)]^2 - [\hat{\sigma}_x + \sigma_x(t)][\hat{\sigma}_y + \sigma_y(t)] + 3[\hat{\tau}_{xy} + \tau_{xy}(t)]^2} \tag{15}$$

Given circular frequency ω, one needs to calculate the superposed stress tensor for each element. Then, the Von Mises stress over a period of $\theta = \omega t \in [0, 2\pi)$ must be calculated and the maximum value for each element stored. This operation has to be repeated over the frequency

Table 8 Example of Von Mises stress with static and dynamic superposition results and errors

Method	Exact	Method	Method	Method C $(\pm\lvert\sigma_x\rvert\pm\lvert\sigma_y\rvert\pm\lvert\tau_{xy}\rvert)$							
	Max	A	B	(+ + +)	(+ + -)	(+ - +)	(+ - -)	(- + +)	(- + -)	(- - +)	(- - -)
$\bar{\sigma}_{vm}$ [MPa]	414	353	471	212	160	353	325	444	421	342	312
$\bar{e}_{vm}[\%]$	---	-14.7	13.8	-48.8	-61.3	-14.6	-21.4	7.3	1.9	-17.4	-24.5

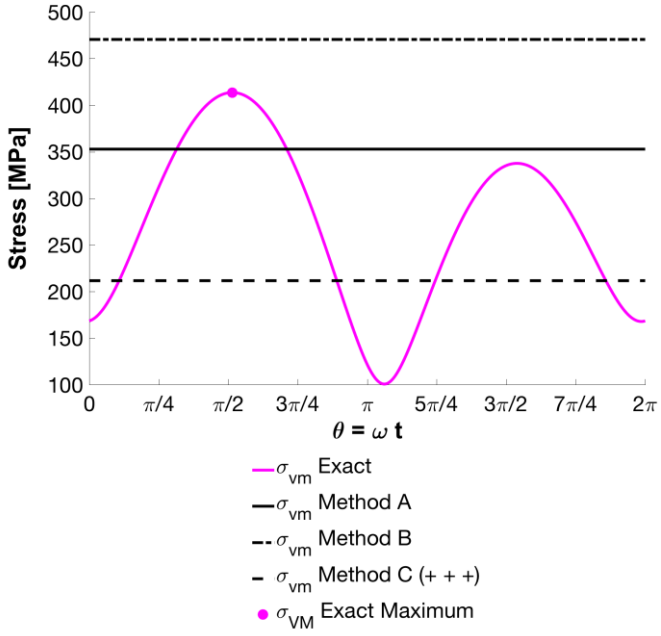

Fig. 9 View of the Von Mises stress with static and dynamic superposition calculation

range of analysis yielding the maximum Von Mises stress. This method, although expensive in matter of time and computation costs, gives the exact value of Von Mises stress.

4.1 Simplified methodologies and analytical example

Since the implementation and use of Eqs. (14) and (15) is very expensive, it is common to make assumptions and simplify the calculation of the Von Mises stress. Several simplified possibilities are evaluated in this section and described in Eqs. (16), (17) and (18). The aim of this section is to evaluate the error in the Von Mises stress calculation when using these simplified methods with respect to the exact Von Mises using Eq. (15).

A The superposed Von Mises stress is the result of the sum of the static Von Mises stress (Eq. (12)) and the dynamic Von Mises stress. The latter does not include the phase information (Eq. (4))

$$\bar{\sigma}_{vm\ A} = \hat{\sigma}_{vm\ static} + \sigma_{vm\ amp} \tag{16}$$

B The superposed Von Mises stress is calculated as the sum of the static Von Mises stress (Eq. (12)) and the maximum dynamic Von Mises stress making use of the phase information (Eqs. (2) and (3))

$$\bar{\sigma}_{vm\ B} = \hat{\sigma}_{vm\ static} + \sigma_{vm}\left(\theta_{\max}\right) \tag{17}$$

C The superposed Von Mises stress is calculated as in Eq. (15) but neglecting the phase information of the dynamic responses

$$\bar{\sigma}_{vm\ C} = \sqrt{(\hat{\sigma}_x \pm |\sigma_x|)^2 + (\hat{\sigma}_y \pm |\sigma_y|)^2 - (\hat{\sigma}_x \pm |\sigma_x|)(\hat{\sigma}_y \pm |\sigma_y|) + 3(\hat{\tau}_{xy} + |\tau_{xy}|)^2} \tag{18}$$

Note that as mentioned in ECSS (2013), Eq. (18) has multiple combinations depending on the sign of the dynamic stresses.

The error is computed as in Eq. (19)

$$\bar{e}_{vm}[\%] = \frac{\bar{\sigma}_{vm\ A,B,C} - \bar{\sigma}_{vm\ exact\ \max}}{\bar{\sigma}_{vm\ exact\ \max}} \cdot 100 \tag{19}$$

As an example, consider the dynamic stress tensor presented in Table 2 and the static stress tensor in Eq. (20)

$$[\hat{\sigma}] = \begin{bmatrix} -120 & +20 \\ & -60 \end{bmatrix} \text{MPa} \tag{20}$$

If one calculates the Von Mises stress considering static and dynamic loads for all the methodologies presented in Eqs. (15) to (18) and calculates the error, one yields the results presented in Table 8. A plot of the Von Mises stress over one period is shown in Fig. 9. Note that for Method C (Eq. (18)), only the combination $(+|\sigma_x|+|\sigma_y|+|\tau_{xy}|)$ is depicted.

4.2 Benchmark example

Consider the tube benchmark example presented in sec. 2. The model is statically loaded with a force of 10 kN applied on the tip mass element. The load is applied in Y direction as depicted in Fig. 10. The Von Mises stress distribution which results after application of the static load case is also shown in Fig. 10.

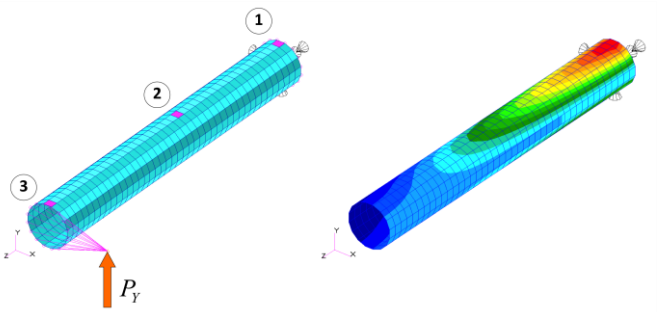

Fig. 10 Overview of the FEM benchmark model static load case and Von Mises stress

Tables 9, 10 and 11 present the results of the Von Mises stress after static and dynamic superposition using the methodologies described in Eqs. (14) to (18) and the errors made using Eq. (19). The superposition is performed with the dynamic stress tensors of the three modes calculated in sec. 3.

Table 9 Element 1 benchmark example static and dynamic Von Mises stress superposition results & errors

Element 1												
Mode	Method /	Exact	Method	Method	Method C $(\pm\lvert\sigma_x\rvert \pm\lvert\sigma_y\rvert \pm\lvert\tau_{xy}\rvert)$							
	Value	Max	A	B	(+ + +)	(+ + -)	(+ - +)	(+ - -)	(- + +)	(- + -)	(- - +)	(- - -)
1	$\bar{\sigma}_{vm}$ [MPa]	901	899	915	135	262	159	275	872	901	861	889
	$\bar{e}_{vm}[\%]$	---	-0.20	1.53	-85.0	-71.0	-82.4	-69.5	-3.14	0.003	-4.46	-1.28
2	$\bar{\sigma}_{vm}$ [MPa]	528	561	554	386	414	378	407	540	561	527	548
	$\bar{e}_{vm}[\%]$	---	6.17	4.76	-27.0	-21.6	-28.5	-23.0	2.18	6.12	-0.24	3.80
3	$\bar{\sigma}_{vm}$ [MPa]	648	651	660	289	296	289	296	648	651	643	646
	$\bar{e}_{vm}[\%]$	---	0.52	1.82	-55.3	-54.2	-55.4	-54.3	0.001	0.49	-0.80	-0.31

Table 10 Element 2 benchmark example static and dynamic Von Mises stress superposition results & errors

Element 2												
Mode	Method /	Exact	Method	Method	Method C $(\pm\lvert\sigma_x\rvert \pm\lvert\sigma_y\rvert \pm\lvert\tau_{xy}\rvert)$							
	Value	Max	A	B	(+ + +)	(+ + -)	(+ - +)	(+ - -)	(- + +)	(- + -)	(- - +)	(- - -)
1	$\bar{\sigma}_{vm}$ [MPa]	645	645	646	67.5	270	68.2	270	590	645	589	644
	$\bar{e}_{vm}[\%]$	---	-0.06	0.09	-89.5	-58.2	-89.4	-58.2	-8.56	0.003	-8.72	-0.15
2	$\bar{\sigma}_{vm}$ [MPa]	343	384	376	211	269	211	269	339	378	339	378
	$\bar{e}_{vm}[\%]$	---	12.0	9.71	-38.5	-21.4	-38.5	-21.4	-1.17	10.3	-1.20	10.3
3	$\bar{\sigma}_{vm}$ [MPa]	311	311	312	274	283	272	281	303	311	301	310
	$\bar{e}_{vm}[\%]$	---	-0.29	0.20	-12.0	-9.08	-12.6	-9.64	-2.64	0.007	-3.23	-0.57

4.3 Discussion on the static and dynamic load superposition

The results of both analytical and benchmark examples show that the simplified methodologies for static and dynamic superposition of Von Mises stresses can produce very conservative or non-conservative results. It is proven that simplified superposition methods are completely case dependent.

The complexity of the structure and its dynamic behaviour together with the way the static and dynamic load are applied are key factors which increase the uncertainty of simplified methods.

Therefore, it is recommended to use the exact approach for the static and dynamic superposed Von Mises stress calculation despite the expensive costs of computation.

Table 11 Element 3 benchmark example static and dynamic Von Mises stress superposition results & errors

Element 3												
Mode	Method /	Exact	Method	Method	Method C $(\pm\lvert\sigma_x\rvert\pm\lvert\sigma_y\rvert\pm\lvert\tau_{xy}\rvert)$							
	Value	Max	A	B	(+ + +)	(+ + -)	(+ - +)	(+ - -)	(- + +)	(- + -)	(- - +)	(- - -)
1	$\bar{\sigma}_{vm}$ [MPa]	274	287	291	148	268	153	271	158	274	152	271
	$\bar{e}_{vm}[\%]$	---	4.76	6.22	-46.0	-2.02	-44.2	-1.01	-42.4	0.001	-44.5	-1.16
2	$\bar{\sigma}_{vm}$ [MPa]	157	172	165	55.1	161	55.3	161	59.9	163	59.7	163
	$\bar{e}_{vm}[\%]$	---	9.52	4.98	-64.9	2.71	-64.8	2.75	-61.8	3.79	-62.0	3.74
3	$\bar{\sigma}_{vm}$ [MPa]	301	357	368	278	285	289	296	294	301	283	290
	$\bar{e}_{vm}[\%]$	---	18.9	22.6	-7.47	-5.05	-3.98	-1.65	-2.29	0.001	-6.0	-3.61

5. Application in spacecraft programmes

Mechanisms are structures which are usually preloaded during launch to keep them in stowed position. In some cases, this preload can be very high and requires to be correctly taken into account in combination with the launch dynamic environment. Also, tubing assemblies often require the addition of internal pressure effects and static enforced displacements to the dynamic motion. In the Structural Engineering department of Airbus DS GmbH Friedrichshafen, we have applied static and dynamic superposition methodologies in several programmes.

A first case of application is the tubing assembly of the MTG propulsion system which requires taking into account internal pressure effects and enforced displacement load cases (see Fig. 11).

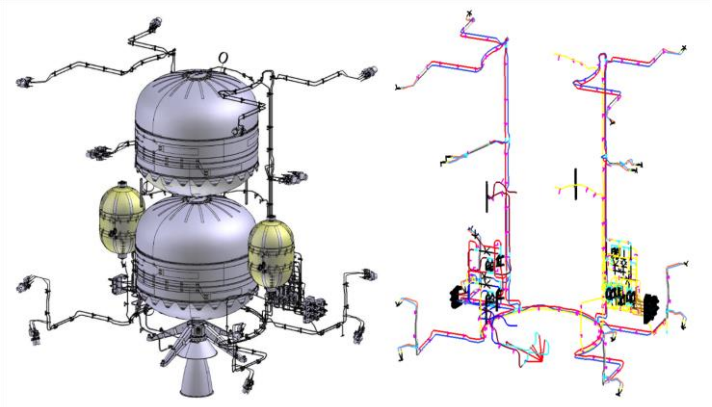

Fig. 11 MTG propulsion system and FEM of the tubing assembly

The most recent application of static and dynamic load superposition within Airbus DS GmbH Friedrichshafen is for a Scan Mechanism (SCM) of the MetOp Second Generation programme (see Fig. 12).

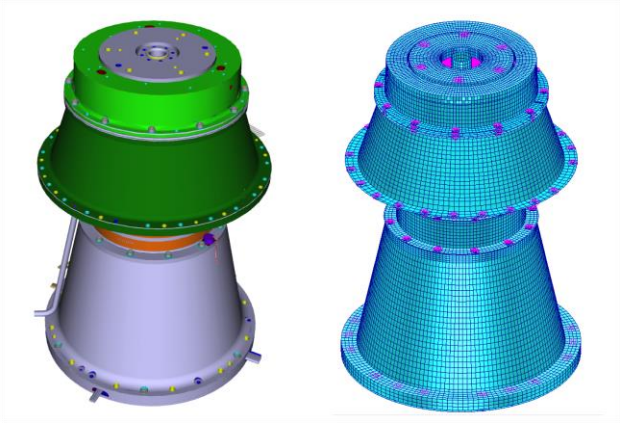

Fig. 12 View of the MetOp Second Generation Scan Mechanism design and FE Model

The methodology followed for the extraction of Von Mises stresses taking into account simultaneously static and dynamic load cases is depicted in Fig. 13. The exact methodology described in Eqs. (14) and (15) was applied. The result was the maximum Von Mises stress after static and dynamic superposition for all elements in the SCM FE model. This procedure, although expensive in matter of computation costs, provided exact Von Mises stress values and hence suppressed the risk of producing very conservative or non-conservative results due to simplifications.

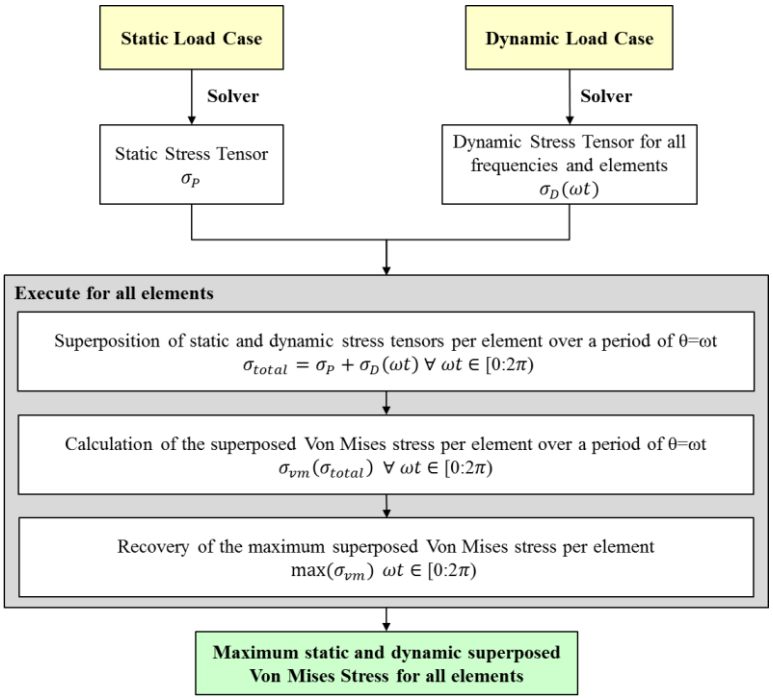

Fig. 13 MetOp SG SCM static and dynamic superposition process followed in Airbus DS GmbH

6. Future perspectives

This paper focused only in harmonic environment. However, in many cases, static loads need to be applied in a random environment. Superposition methodologies for static and stochastic loads require a greater degree of study.

In addition, this study has mainly referred to the calculation of Von Mises stresses and resultant forces. Nevertheless, there are many other situations where the impact of the phase of the responses and of methods for static and dynamic load superposition need to be studied and derived. Table 12 highlights some of these situations.

Table 12 Overview of potential situations for static and dynamic superposition studies

Analysis Case	Context	Application
Stress Analysis	Metallic	Von Mises Stress Principal Stress
	Composite	Failure Indexes Wrinkling Dimpling Crimping Core rupture
Joints Analysis	Bolted Joints	Shear failure Bearing failure Slippage
	Inserts	Tensile failure Shear-out failure
Notching	Forces	Combined forces
	Accelerations	Combined accelerations

7. Conclusions

In this paper, methodologies for static and dynamic load superposition have been discussed in the framework of harmonic environment. Analytical and FE based examples have been provided for the calculation of Von Mises stress. The results of the comparison between exact and simplified methodologies show that simplified methodologies lead to very conservative and non-conservative results. Besides, it is difficult to know the degree of conservatism or non-conservatism without knowing the exact value beforehand.

The importance of the phase of the responses in dynamic analysis has been discussed. It has been proven that ignoring the phase information in the calculation of Von Mises stresses leads to very conservative or non-conservative results. It has also been demonstrated that in the calculation of resultant forces, one always yields conservative results if the phase information is ignored.

To conclude, in order to obtain accurate results in dynamic response combination, exact methodologies which take into account the phase of the responses should be used. In addition, for static and dynamic load superposition cases, it is essential to use an exact methodology since simplified methodologies may lead to very conservative or non-conservative results.

There are many scenarios where dynamic load combination and static and dynamic load superposition may be necessary. Some of these potential scenarios have been identified in this

paper. It is important to keep in mind these scenarios and evaluate the risks/impact when using methods which ignore the phase of responses.

For simplification, 2D force vectors and stress tensors have been used in this study. The superposition methodologies and the conclusions presented in this paper are also applicable in a 3D environment.

References

Charron, F., Donato, L. and Fontaine, M. (1993), "Exact calculation of minimum margin of safety for frequency response analysis stress results using yielding or failure theories", *Proceedings of the 1993 MSC World Users' Conference*

ECSS (2013), *ECSS Space Engineering-Spacecraft Mechanical Loads Analysis Handbook*, ECSS-E-HB-32-26A, 19th February 2013.

CC